energies

MDPI

Article

Modelling an Influence of Solar Cells' Connection Manner in Silicon Photovoltaic Modules on Their Characteristics with Partial Shading

Krzysztof Górecki *, Ewa Krac and Jacek Dąbrowski

Department of Power Electronics, Gdynia Maritime University, Morska 83, 81-225 Gdynia, Poland; e.krac@we.umg.edu.pl (E.K.); j.dabrowski@we.umg.edu.pl (J.D.)
* Correspondence: k.gorecki@we.umg.edu.pl

Abstract: The article considers the problem of an influence of partial shading on the characteristics of photovoltaic modules (PV modules). Different manners of connections of silicon solar cells contained in such modules are considered, e.g., classical PV modules (I and II generation of modules) and modules made using half-cut technology (III generation of modules). A model of PV modules was proposed. This model has the form of a network for the SPICE program and takes into account the influence of partial shading of the PV module caused by clouds or terrain and architectural obstacles on its current and voltage. The form of the model was described, and the DC characteristics of the considered classical and half-cut modules, calculated using the formulated model, were compared to the measurement results under different shading conditions. Some calculations using the proposed model were performed for different methods to connect solar cells in PV modules. The obtained results were discussed.

Keywords: photovoltaic modules; modelling; SPICE; measurements; shading of PV modules; DC characteristics

Citation: Górecki, K.; Krac, E.; Dąbrowski, J. Modelling an Influence of Solar Cells' Connection Manner in Silicon Photovoltaic Modules on Their Characteristics with Partial Shading. *Energies* **2024**, *17*, 5741. https://doi.org/10.3390/en17225741

Academic Editor: Isabel Jesus

Received: 25 October 2024
Revised: 13 November 2024
Accepted: 14 November 2024
Published: 16 November 2024

1. Introduction

Photovoltaic (PV) installations are a commonly used alternative source of electrical energy [1,2]. The basic components of such installations are PV modules containing interconnected solar cells and diodes protecting these cells against incorrect connection of the module to other components of the PV installation [2,3]. As it is known [4–8], the efficiency of a photovoltaic installation strongly depends on atmospheric conditions, including solar irradiation. It changes with the time of day and the season [6,8–11]. The consequence of these changes is the variable efficiency of the considered installations during the day and in different seasons of the year [6].

In the morning and evening, when PV modules are irradiated by radiation with a lower power density value, the amount of electricity produced by such installations is much lower than at noon, when the operating installations are exposed to the maximum irradiation for a given day and region [6]. Similarly, PV installations produce much less electricity in the autumn and winter months, when the days are short, and PV modules are less irradiated than in the spring and summer months [6].

In addition, the value of the power density of light irradiating the operating PV modules is influenced by cloud cover and shadows caused by the occurrence of terrain obstacles such as a tree, chimney, or building located in the vicinity of the operating PV installation [7]. This additionally adversely affects the operation of such installations [12–15].

As a result, the amount of electricity generated in periodically shaded PV installations is much smaller than it would be, resulting from the energy yield forecasts assuming the specific constant peak power of the PV installation. Apart from the fact that this brings measurable losses to the owners of photovoltaic installations, it also makes it difficult to

forecast the amount of energy produced by the considered installations during the day, month, quarter, or year. Hence, there is a need to conduct work on new concepts for increasing the productivity of PV modules and on the development of PV module models that would allow the daily, monthly or annual electricity production to be forecast for the considered PV modules, taking into account the occurrence of permanent or variable obstacles on the radiation illuminating photovoltaic modules.

Since the launch of the first photovoltaic installation, continuous work has been carried out on improving the productivity of the considered solutions [15,16]. As a result of this work, new technologies are being created, not only for single solar cells [17,18], but also for PV modules operating in PV installations [19]. Currently, regarding commercial solutions used during the construction of PV installations, three generations of such modules can be distinguished.

Typical PV installations contain PV modules and a system based on an inverter that adjusts the generated current and voltage to the ac grid requirements. Additionally, some PV installations are equipped with a subsystem that stores the excess of energy generated [20]. However, the common components for all PV installations are solar cells, which are used to build PV modules installed in both small and large PV installations [2,20].

In the modules considered, the most commonly used are silicon solar cells (PV cells) [1], called the first-generation solar cells. They are characterized by the stable and repeatable technology of production, high efficiency of converting solar irradiation into electricity (up to 23%—Champion Photovoltaic Module Efficiency Chart [21]), and a low loss of efficiency as a function of time. In the first year of the module's life, the efficiency drop is below 2%, and in each subsequent year, it is between 0.5% and 0.6% [22]. The second generation of the considered devices typically contains amorphous and thin film solar cells, whereas the third generation includes such technologies as organic solar cells, dye-sensitized solar cells, Perovskite-based cells, quantum dot solar cells, or tandem solar cells [23]. The third generation includes printed solar cells and organic solar cells. Meanwhile, the efficiency of the commercially available third-generation solar cells is only up to 8%, and the lifespan of organic solar cells does not exceed several months [24].

Just a few years ago, a typical PV module contained 60 or 72 series-connected solar cells (first-generation PV modules). In order to protect the module in question from reverse polarization, which occurs, for example, when one or more of the solar cells in the PV module is shaded, such a panel is equipped with a bypass diode. In order to improve the productivity of working modules, PV modules are equipped with three bypass diodes to protect three subsections of series-connected solar cell strings (second-generation PV modules). Thanks to this, when a solar cell in such a module is shaded, this shading causes a loss of only 1/3 of the electrical energy produced by the PV module.

Another solution improving the reliability of PV modules is the half-cut technology. Typical modules made in this technology contain 120 or 144 halves of solar cells organized in such a way that 60 or 72 half-cut solar cells are connected in series in two parallel connected sub-modules. Additionally, these modules are equipped with three bypass diodes properly connected to such a circuit [25,26]. Thanks to this, when a single solar cell in such a module is shaded, only 1/6 of the operating PV module is switched off [27].

In recent years, many scientists have been involved in modelling both individual photovoltaic cells and PV modules, as well as entire photovoltaic systems [28–36]. These models were formulated using various procedures. They describe photovoltaic cells, photovoltaic modules, or PV systems using a different number of parameters and are characterized by different accuracy levels. The group of such models also includes models dedicated to the SPICE program [6,11,36–39]. SPICE (Simulation Program with Integrated Circuits Emphasis) is dedicated to computer analysis of electronic networks.

For example, the single-diode model of a photovoltaic cell described in [29] takes into account the photocurrent, the diode saturation current, the non-ideal factor of the p-n junction, and the series resistance of the photovoltaic cell. According to the authors of the cited paper, the test results confirm that the model of a photovoltaic cell with one diode is an accurate model for silicon photovoltaic cells; however, as the authors of the paper [29]

admit, a satisfactory agreement between the calculated and measured characteristics was not achieved when the temperature increased. These discrepancies increased as the power delivered to the load increased. Therefore, in [29], it was proposed to use a model with nine diodes. However, this model only allows the error to be reduced when calculating the characteristics of the tested photovoltaic cell at a high temperature.

In [33], a method for modelling PV modules was proposed, taking into account only the parameters of the photovoltaic module provided by the manufacturer. The cited paper indicates the need to take into account the variability of environmental conditions in PV panel models, but the model with one diode proposed in the cited paper only takes into account the possibility of PV modules operating for specific, constant irradiance and temperature conditions. Additionally, this model does not take into account the generation–recombination component of the p-n junction current or a change in the angle of incidence of the rays illuminating the PV cells.

The paper in [25] presents a model of a half-cut module. This model is based on the two-diode solar cell model described in [40], and it does not take into account changes in the temperature inside the photocells during their operation. The authors of [25] state that the proposed model is described by 11 parameters, including the fill factor (FF) and open-circuit voltage (V_{oc}). Moreover, the paper provides neither an analytical representation of the source representing the photocurrent density nor a description of diffusive and recombination components of the p-n junction current. Only the calculations of a power loss due to the losses caused by connecting individual strings of the photovoltaics are shown.

The aim of this article is to investigate the influence of the method of connecting solar cells in a PV module on the resistance of this module to partial shading. A module containing an identical number of solar cells is considered, which are connected in strings with different numbers of solar cells, and each of these strings is bypassed by a semiconductor diode, which allows current to flow when the bypassed string does not produce energy due to shading. A model of the considered modules was formulated in the form of a subcircuit for the SPICE program. Calculations and measurements of the characteristics of PV modules containing the same number of solar cells connected in a different number of strings were carried out. Selected calculation results were verified experimentally. The feasibility of constructing PV modules containing a different number of strings was analysed from the point of view of resistance to partial shading.

Section 2 discusses the construction of PV modules made using the classic and half-cut technology. Section 3 presents the model of a PV module taking into account its partial shading. Section 4 presents the utilized measurement set-up and the tested PV modules. The calculation results obtained using the developed model along with the measurement results are presented and discussed in Section 5. Section 6 contains the results of calculations obtained for different kinds of PV modules operating under different shading conditions.

2. Construction of PV Modules

Until recently, second-generation silicon PV modules of the dimensions 1000 × 1670 × 35 mm were the most popular on the market. They were composed of 60 or 72 solar cells of the same type connected in series, and had the dimensions 156 × 156 mm [25]. Additionally, a series of solar cells was connected to three bypass diodes, dividing the solar cells into three series-bypassed segments containing 20 or 24 solar cells in each string. Each illuminated solar cell in such a module produced a current, the value of which depended, among other things, on the irradiance of the radiation illuminating it. In the case of slight partial shading of a single solar cell, because in such a module the solar cells are connected in series, there was a proportional decrease in the photocurrent value in the entire working chain of solar cells, which significantly reduced the amount of electricity produced.

Additionally, polarity reversal could have occurred in the very shaded solar cell. This means that the shaded solar cell stopped producing electricity and became a load through which current flowed from neighbouring solar cells, illuminated by the radiation with

higher irradiance. The excess energy in the shaded solar cell was released as heat, and places were created in the operating modules where junction temperature increases occurred, i.e., so-called hot spots. In extreme cases, this phenomenon could result in damage to overheated solar cells contained in the PV modules.

In the context of the problems under consideration, a major change was brought about by the introduction of PV modules manufactured using half-cut technology, which has been improved and widely introduced to the market over the last few years. The PV modules manufactured according to half-cut technology operate on a slightly different principle than the classic PV modules, apart from the fact that they contain two parallel chains of solar cell halves connected in series. The structure of the PV module made using the considered technology is shown in Figure 1a. For comparison, in Figure 1b,c, the structures of the modules of II generation and I generation are shown, respectively.

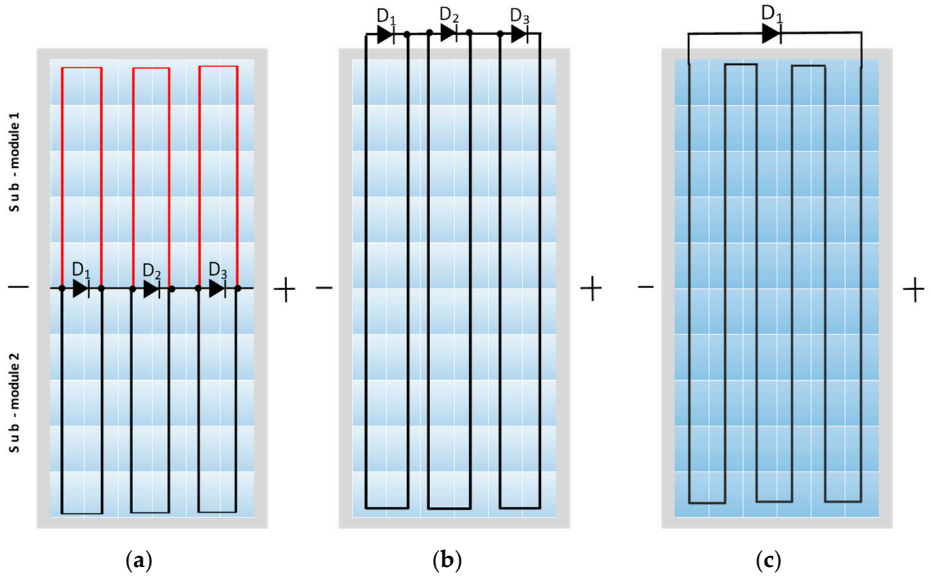

Figure 1. PV modules made using half-cut technology (**a**), module of II generation (**b**), and module of I generation (**c**).

The novelty introduced in half-cut modules consists of dividing individual solar cells in half (in Figure 1a, the intersection of the photocell is symbolically marked with a black dashed line). Hence, such modules contain not 60 or 72, but 120 or 144 solar cells of the size 156 × 78 mm. As a consequence of reducing the surface area of solar cells, the cells contained in one submodule generate a current of lower value than solar cells contained in the modules made using classical technology, while finally maintaining the same clamping current and voltage. Half-cut solar cells allow for a four-fold reduction in power losses on the cell-to-module line (CTM) [3,19,40,41]. Additionally, by halving the current flowing through the cells cut in half entirely in the sub-module, these modules have a much lower operating temperature than PV modules made using classic technology [25]. This additionally increases their efficiency and significantly extends their lifetime [26,40,42–44].

The organization of the solar cells contained in the half-cut modules is also different. Such a module is composed of two sub-modules (chains of solar cells) connected in parallel, as previously mentioned (Figure 1a). Each sub-module contains 60 or 72 solar cells connected in series and three bypass diodes, which additionally divide the solar cell chain into three meanders in each sub-module, with 20 or 24 solar cells in each meander. It is also possible to construct PV modules containing more than two sub-modules connected in parallel to each other and different numbers of bypass diodes. Such a module can be more resistive for partial shading, but its construction is more complicated. Analyses of the properties of different constructions of such modules are presented in the next sections.

3. Model Form of PV Modules

The proposed PV module model was developed based on the solar cell model, which is a modified version of the model proposed in the papers [39,45]. A network representation of this solar cell model is shown in Figure 2.

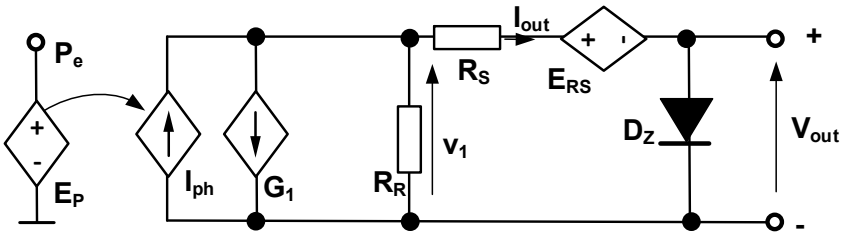

Figure 2. Network representation of the solar cell model.

The considered model of a solar cell consists of a controlled voltage source E_P, representing irradiation on the surface of the solar cell. The controlled current source I_{ph} describes the photocurrent generated in the solar cell. The controlled current source G_1 describes the current–voltage characteristic of the p-n junction contained in the solar cell. The resistor R_R models the leakage current of the solar cell, whereas the resistor R_S and controlled voltage source E_{RS} describe the series resistance of this cell. The diode D_Z is used to model the breakdown phenomena in the solar cell. This diode is described using the built-in model of the diode in SPICE, e.g., in [46]. In order to limit the influence of this diode on the characteristics of the solar cell operating in its typical operating area, the values of the model parameters of this diode are selected in such a way that the forward voltage of this diode is much higher than forward voltage of the p-n junction of the solar cell. I_{out} and V_{out} denote the current of the solar cell and the voltage of this cell, respectively.

The same network form as presented in Figure 2 has the model of a string of solar cells containing m solar cells connected in series. For such a string, the particular components visible in Figure 2 are described with Equations (1)–(3). Upon formulation of these equations, it was assumed that all the solar cells contained in the modelled string were the same.

The controlled voltage source E_P represents the irradiance on the string of the solar cell surface. The controlled current source I_{ph} describes the photocurrent using the formula of the form:

$$I_{ph} = P_e \cdot m \cdot S \cdot SR \cdot x \tag{1}$$

where P_e is the irradiance on the solar cell surface, S is the active surface of the solar cell, m is the number of solar cells in the string, SR is the current sensitivity of the solar cell, and x is a binary variable representing the shading of any cell in the string (x = 0) or the lack of shading (x = 1).

The controlled current source G_1 models the I-V characteristics of the p-n junctions connected in series in the string using the formula of the form:

$$I_1 = J_o \cdot S \cdot \left(\frac{T_j}{T_0}\right)^3 \cdot \exp\left(-\frac{U_{go}}{n \cdot k/q \cdot T_j}\right) \cdot \left[\exp\left(\frac{v_1}{m \cdot n \cdot k/q \cdot T_j}\right) - 1\right] \tag{2}$$

where J_0 denotes the parameter of saturation current density, n is the emission factor of the p-n junction, U_{go} is the voltage corresponding to the band-gap of silicon, v_1 is the voltage on the controlled current source G_1, k is the Boltzmann's constant, q is the electron charge, T_j is the junction temperature, and T_0 is the reference temperature.

The controlled voltage source E_{RS} models the influence of junction temperature on the equivalent series resistance of the solar cell by the linear dependence of the form:

$$E_{RS} = V_{RSO} \cdot \alpha_{RS} \cdot (T_j - T_0) \tag{3}$$

where α_{RS} denotes the temperature coefficient of series resistance, and V_{RSO} is the voltage on resistor R_S. The value of R_S resistance is equal to the product of the number m and the series resistance of the solar cell. Temperature T_j is the sum of the ambient temperature and a temperature increase caused by the conversion of light into heat. The values of parameters occurring in the solar cell model were estimated using the idea of local estimation described, e.g., in [35].

The model of the photovoltaic module has a form of serial–parallel connection of the models of strings of solar cells described above and the models of bypass diodes built into the SPICE program. For example, for classical PV modules of the first generation, such a model contains a model of one string of solar cells connected in series with one bypass diode. In turn, the network representation of the half-cut PV module is shown in Figure 3.

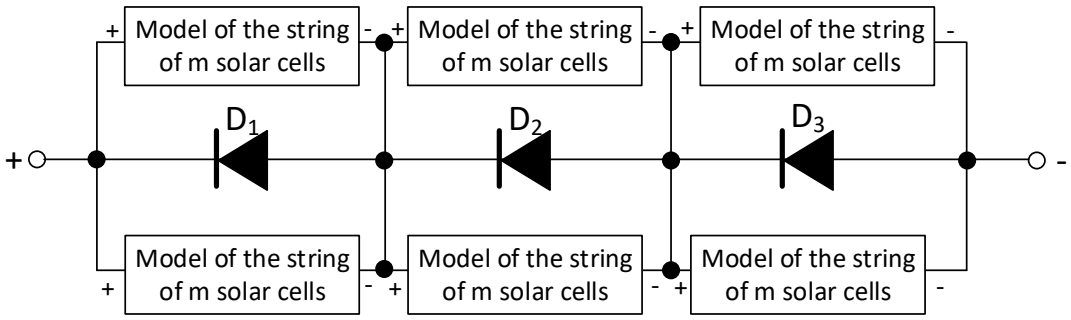

Figure 3. Network representation of the electrothermal model of the half-cut PV module.

In the presented PV module model, the bypass diodes were modelled using the model built into the SPICE program and described, among others, in the book [46]. The model of the string of m solar cells has the form shown in Figure 2 and is described by Equations (1)–(3). The parameter x concerns the most shaded photocell in the chain.

If no solar cell is shaded, only a small reverse (leakage) current flows through diodes D_1–D_3. If a cell is shaded, the appropriate diodes shunt a specific string of solar cells, and the current generated in the unshaded strings flows through them.

If the number of diodes and strings connected in parallel is different than that shown in Figure 3, the structure of the model should contain proper (physical) numbers of bypass diodes and strings of solar cells.

4. Measurement Set-Up

To verify the correctness of the formulated model of the PV module and investigate the influence of partial shading of the properties of such modules with different constructions, measurements of the characteristics of the considered module were carried out, fully illuminated by radiation and taking into account partial shading, and then compared to the characteristics calculated using the formulated model. For this purpose, a measurement set-up was designed and constructed. A diagram of this set-up is shown in Figure 4.

This set-up consists of a light-tight testing chamber and a block of control and recording measurement results. The testing chamber is designed to enable full control of the lighting conditions of the tested PV module and uniform distribution of radiation over its entire surface. It contains the tested PV module, a light source generating radiation illuminating the tested PV module, and a photoradiometer sensor. In the measurement set-up under consideration, the source of optical radiation is a halogen lamp. Additionally, the radiation source, the tested device, and the photoradiometer sensor are placed in a light-tight chamber, thus preventing excessive scattering of the light illuminating the tested PV module.

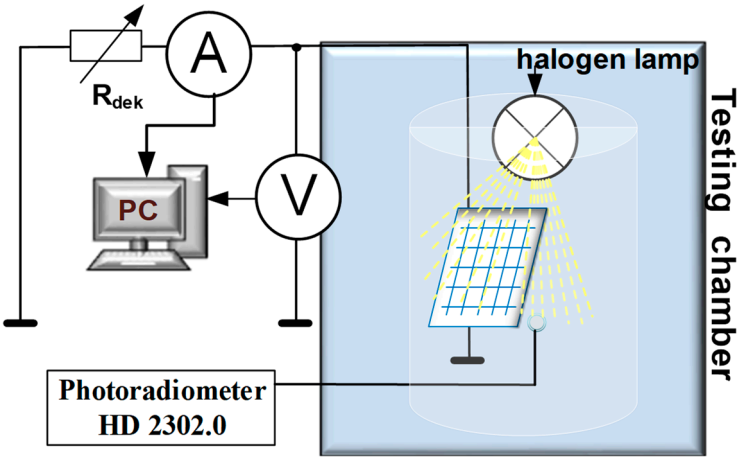

Figure 4. Diagram of the measurement set-up.

The block of control and recording measurement results was equipped with a computer recording the measurement results, as well as a Rigol DM3068 (by Rigol Technologies, Beijing, China) voltmeter (V), a Rigol DM3068 ammeter (A), a load resistor (R_{dek}), and an HD 2302.0 photoradiometer (by Senseca Italy Srl, Selvazzano Dentro, Italy) to record irradiance on the surface of the tested module. The voltmeter and ammeter were equipped with a USB interface that allowed the measurement results to be transferred directly to a computer. After measuring the characteristics of the tested module, they were compared to the characteristics calculated using the formulated model of the considered PV module.

The measurements were carried out for PV modules constructed by the authors. All these modules contained 60 polycrystalline photovoltaic cells of the type 1713847-velleman-sol1n [47], with the dimensions 46 × 40 mm and rated power of 0.2 W. These cells were placed on a flat substrate, cell to cell. A view of the assembled module is shown in Figure 5.

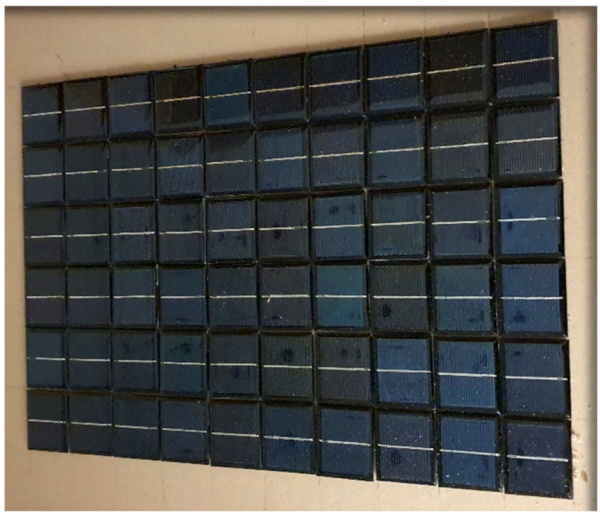

Figure 5. View of the tested half-cut module.

Different kinds of connections of the solar cells into strings were considered. We considered three constructions of the tested PV modules. The first of them (module I) consisted of one string of 60 solar cells connected in series and one bypass diode. The second PV module (module II) consisted of three strings of 20 solar cells connected in series. Each string was bypassed by one diode. The last PV module (module III) was constructed according to the half-cut topology. It contained six strings of 10 solar cells connected in series and three bypass diodes. All these diodes were connected with solar cells according to Figure 1, and parallel to each diode, two strings of solar cells were connected. In each of

the tested modules, the diodes of the type 1N5817 [48] were used as a bypass of each string of solar cells.

5. Investigations Results

Using the model presented in Section 3, the current–voltage characteristics of the solar cell contained in the considered module and the entire module were calculated with various variants of its partial shading and then compared to the measured characteristics. Shading of individual solar cells from the tested module was carried out by covering their surfaces with a black screen impermeable to optical radiation. In the following figures, the calculation results are marked with lines, and the measurement results are marked with points.

Figure 6 illustrates the calculated and measured characteristics of a single solar cell with irradiance on its surface of about 480 W/m^2.

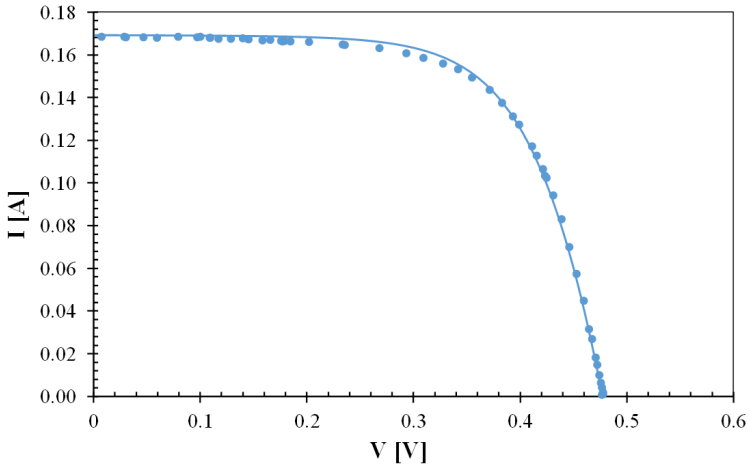

Figure 6. Calculated and measured characteristics of the solar cell used to construct the tested module at irradiance of 480 W/m^2.

As can be seen, a very good agreement between the calculation and measurement results was obtained. The differences between these results did not exceed 2.5%. As a result of illuminating the solar cell with a halogen lamp, its temperature increased to 44 °C (at ambient temperature equal to 22 °C), which was taken into account in the calculations. The obtained short-circuit current value of 170 mA was lower than the rated value of the solar cell current due to the lower than standard irradiance value. The open circuit voltage was equal to 0.48 V.

Figure 7 shows the current–voltage characteristics of the tested modules without shadows at an irradiance of about 400 W/m^2.

As can be seen, the shape of the module's characteristics was similar to the shape of the characteristics of a single solar cell. The value of the short-circuit current for modules I and II reached about 140 mA, whereas for the module III, it reached about 280 mA. The value of this current for module III was about twice as high as that for the other modules, because module III contained two strings of solar cells connected in parallel, whereas in the other modules, only one such string existed. The open circuit voltage was equal to 14.5 V for the module III and about 29 V for the other modules. The observed differences between the voltages obtained for the considered modules were a result of different numbers of solar cells connected in series in particular modules. The differences between the characteristics obtained for modules I and II were very small, and they were a result of small differences in ambient temperature during the performed measurements. Differences between the results of the measurements and calculations were acceptable, and they did not exceed 7%. Figure 8 presents the dependence of power produced by the considered modules on the voltage of the module.

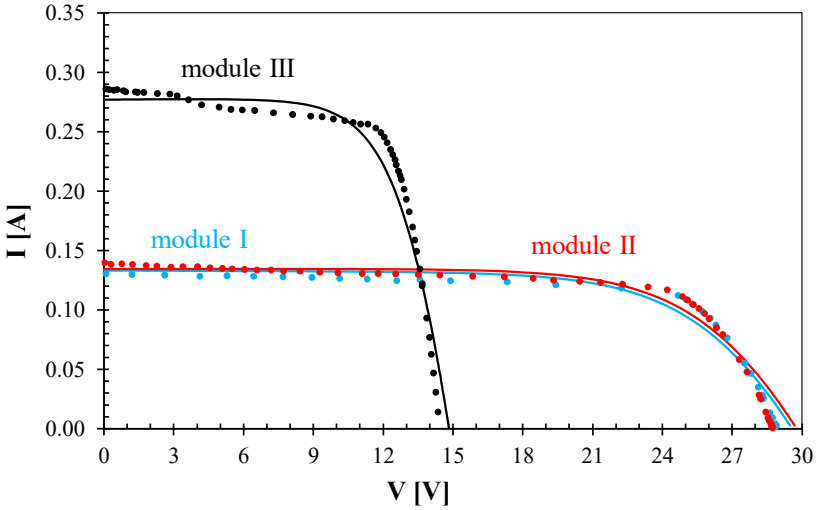

Figure 7. Calculated and measured characteristics of the tested modules with no shading of their surfaces.

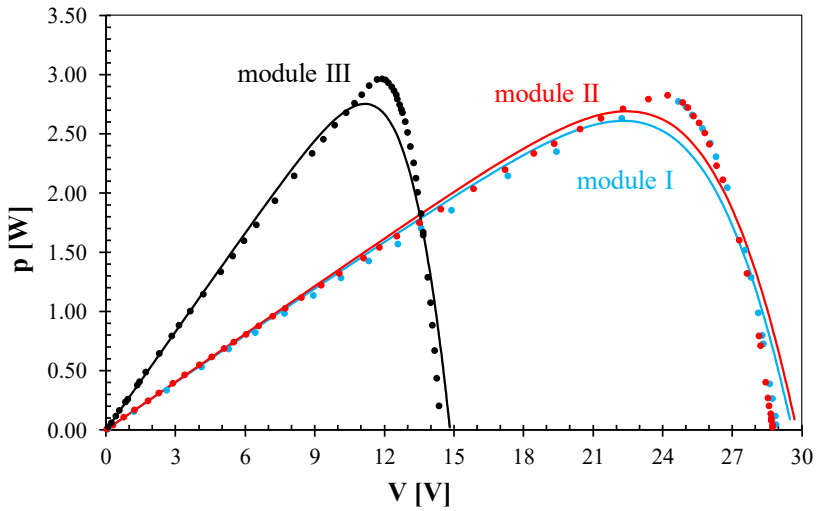

Figure 8. Calculated and measured dependences of power produced by the tested modules on the voltage of the tested modules operating with no shading of their surfaces.

As is visible, the maximum value of power was obtained for module III. It was equal to 3 W. This maximum was observed at a voltage equal to 12 V, whereas for modules I and II, the maximum was observed at a voltage equal to 24.5 V. The differences in the maximum values of power for the considered modules did not exceed 5%.

The following figures illustrate the impact of shading various parts of the tested module on its current–voltage characteristics. In each figure, in addition to the designated characteristics, it is illustrated (by blackening) which solar cells and which strings were covered during the measurements. The description uses the letters A, B, and C (bottom half of the module) and D, E, and F (top half of the module) to designate these strings in module III. This is illustrated in Figure 9. For modules I and II, the strings are denoted with letter A (module I) and with the letters A, B, and C (module II).

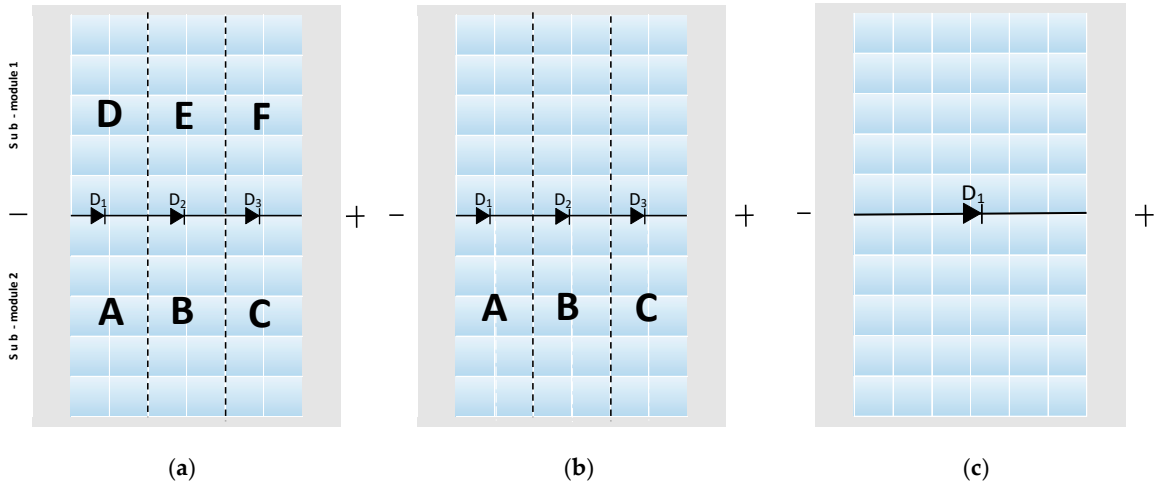

Figure 9. Method for determining meanders in the tested half-cut module (**a**), module II (**b**), and module I (**c**).

Figure 10 illustrates the modules' characteristics in a case where only one solar cell in string A is covered.

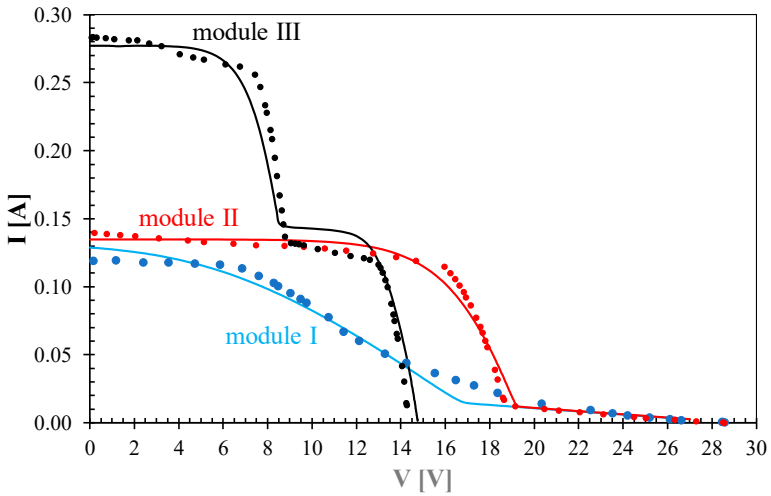

Figure 10. Calculated and measured characteristics of the tested module when one solar cell is shaded in meander A.

According to the simple theory, if any solar cell in module I is shaded, no current should flow through this module. However, it is visible that, with a small value of the voltage module, the current of the value, even exceeding 0.1 A, flowed through this module. This was a result of a breakdown phenomenon occurring in the shaded solar cell. The small slope of the I-V characteristic in the range of voltage V > 19 V corresponded to the leakage resistance R_R of the solar cell. The effect of the breakdown of the solar cell was visible for module I because the breakdown voltage had a lower value than the maximum value of voltage produced in one string of solar cells connected in series. In turn, in module II, the mentioned phenomenon was not visible. For this module, it was easy to observe that, due to the shading of one solar cell, the maximum voltage value, at which the current was higher than 0.1 A, was reduced to only 17 V, whereas for the non-shaded solar cell in this module, this voltage was equal to 26 V (see Figure 7). The visible shape of the module II characteristic was a result of the use of a bypass diode, which was connected in parallel to the string containing the shaded solar cell. The characteristic obtained for module III had a different shape than that of the characteristics visible for the other modules. For this module, which operated with one shaded solar cell, the full current load could only be

achieved for a voltage below 8 V. However, with a current twice as low as the short-circuit current, it was possible to obtain a voltage above 13 V. The value of the open circuit voltage was approximately 15 V. The visible shape of the considered characteristic was a result of strings connected in parallel containing shaded and non-shaded solar cells. Due to the use of the non-shaded strings of solar cells, a path of current conduction existed in the module.

Another example, illustrated in Figure 11, concerns the case in which one solar cell located in meander A and one solar cell located in meander B were covered.

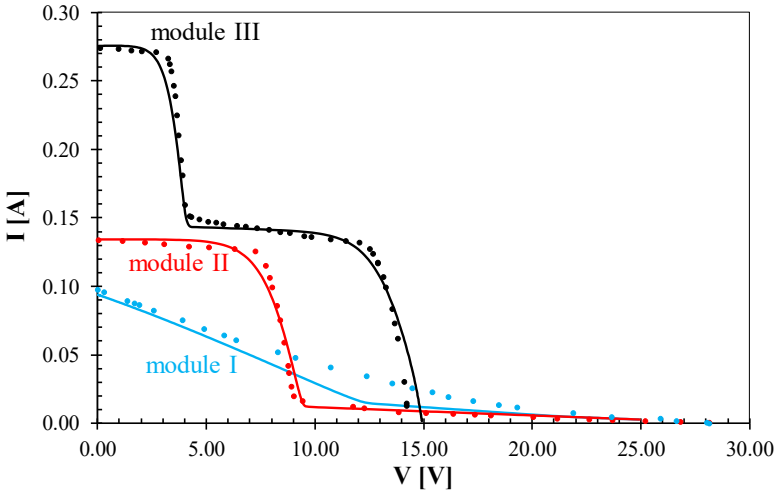

Figure 11. Calculated and measured characteristics of the tested module when shading one solar cell in string A as well as in string B.

The shapes of the characteristics presented in this figure are similar to the characteristics presented in Figure 10, but the range of values of the module voltage, at which the high values of the module current were observed, is narrower. For module I, the current was a decreasing function of the voltage. For V > 12 V, only the leakage current flowed through this module. In turn, for module II, the short-circuit current could be observed for voltage V < 8 V. For module III, one can see that the value of the open circuit voltage decreased due to the fact that chains A and B did not produce currents. They were shunted by the bypass diodes. The short-circuit current could be observed only for the voltage V < 4 V. A current equal to the half of this current could be obtained for voltage V < 14 V.

Figure 12 shows the characteristics of the tested modules when shading the solar cells contained in strings A, B, and C.

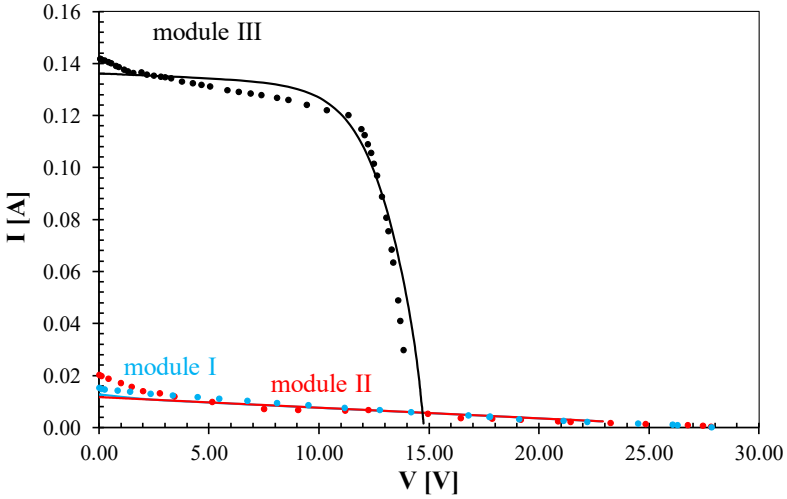

Figure 12. Calculated and measured characteristics of the tested modules when shading solar cells in strings A, B, and C.

For modules I and II, the current flowed through the leakage resistance of the shaded solar cells. In turn, for module III, the shape of the I-V characteristics was similar to that for the module operating without any shading. Only the value of the short current was twice as low as that for the module operating without any shading. For all the modules, good accuracy was obtained between the results of the measurements and the calculations.

Figure 13 shows a comparison of the dependences of the power generated in module I (Figure 13a), in module II (Figure 13b), and in module III (Figure 13c) on the module voltage with different numbers of shading solar cells. The worst case is considered as the scenario in which the shaded solar cells are situated in strings connected in series. In this figure, the brown colour corresponds to a non-shaded module (curve 1), the red colour corresponds to one shaded solar cell (curve 2), the black colour corresponds to two shaded solar cells (curve 3), and the blue colour (curve 4) corresponds to three shaded solar cells.

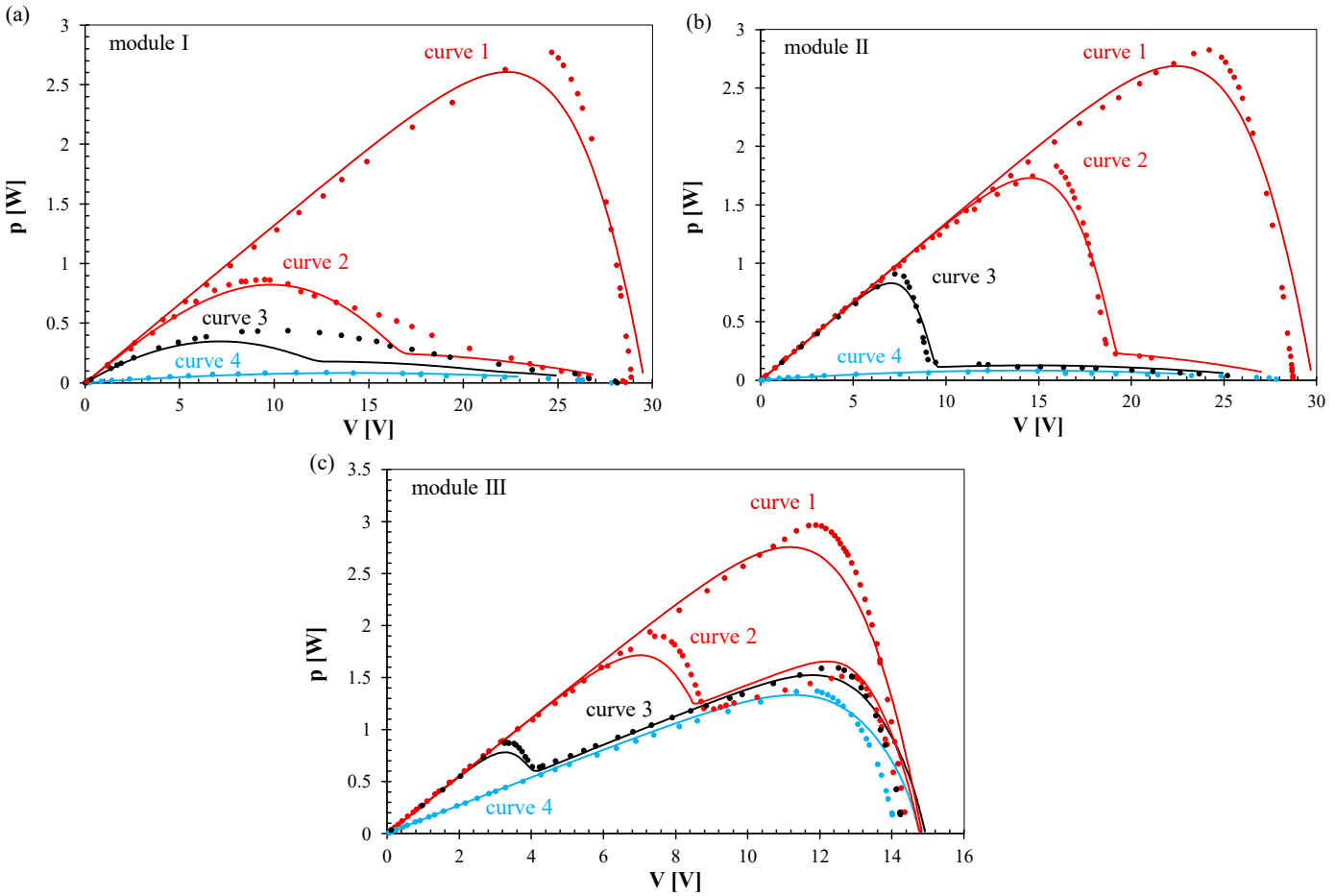

Figure 13. Calculated and measured dependences of power produced by the tested variant modules under different shading conditions on the modules' voltages: (**a**) module I, (**b**) module II and (**c**) module III.

As can be observed, the maximum power produced by all the considered modules operating without any shading had the same values. If one solar cell was shaded, module I produced a power twice as low as that of modules II and III. With two shaded solar cells, the largest maximum value of the produced power was observed for module III, whereas the smallest was observed for module I. These values of produced power differed between one another up to four times. If three solar cells were shaded, the maximum power produced by module III was ten times higher than that for the other modules. The presented results show that the use of module III is the most profitable when the number of shaded solar cells is the largest.

In the next section, some other constructions of PV modules are considered. In these modules, the same numbers of solar cells are used, but they are connected with different number of series–parallel-connected strings.

6. Analyses of Properties of Different Construction of PV Modules

Using the model of the PV module described in Section 3, computer analyses of PV modules of different designs were carried out. Each of these designs used 60 solar cells. The analyses assumed that these solar cells were identical. The following variants of connections of these solar cells in the module are considered:

(a) 60 solar cells connected in series in one string and one p-n diode connected antiparallel to the solar cell string (module A);
(b) Three series-connected strings of 20 solar cells, each of which is bypassed by an antiparallel diode (module B);
(c) Two parallel-connected strings containing 30 solar cells each and 1 p-n diode connected antiparallel to the solar cell string (module C);
(d) Three series-connected sets containing two parallel-connected strings containing 10 solar cells each and 3 p-n diodes connected antiparallel to each set (module D);
(e) Six series-connected sets containing two parallel-connected strings containing five solar cells and 6 p-n diodes connected antiparallel to each set (module E);
(f) Five series-connected sets containing four parallel-connected strings containing three solar cells each and 5 p-n diodes connected antiparallel to each set (module F).

The calculations assumed the values of the parameters of individual solar cells corresponding to the actual devices described in Section 2. All calculations were performed for a fixed value of irradiation power density on the panel surface: $P_e = 1\ kW/m^2$. Only the cases of full shading of selected solar cells or no such shading were considered.

Figure 14 shows the calculated dependence of the power produced on the voltage for the tested modules, obtained in the absence of shading of any solar cell in the tested modules.

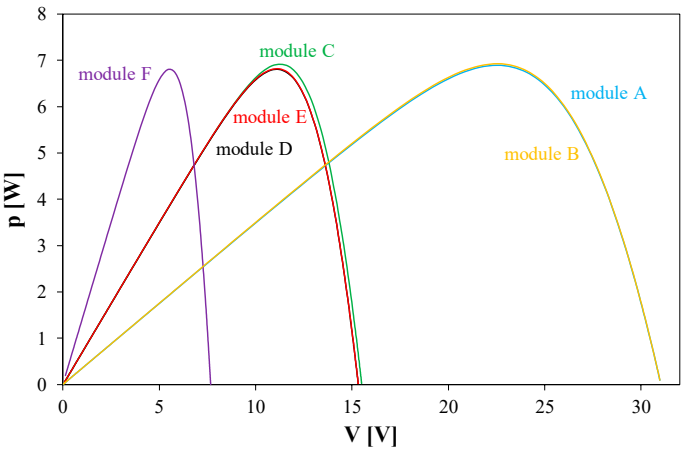

Figure 14. Dependence of the power produced on the voltage for the tested modules in the absence of shading.

As can be seen, there was one maximum on the p(v) characteristic for each module. The maximum value of power generated by the tested modules in the absence of shading was similar for all tested modules. The differences did not exceed 1.5%. It is worth noting that, for modules A and B, the power reached its maximum value at a voltage of about 23 V; for modules C, D, and E, at a voltage of 11 V; and for module F, at a voltage of 5 V.

The case of the influence of shading of one solar cell in the tested modules on their p(v) characteristics is considered in Figure 15.

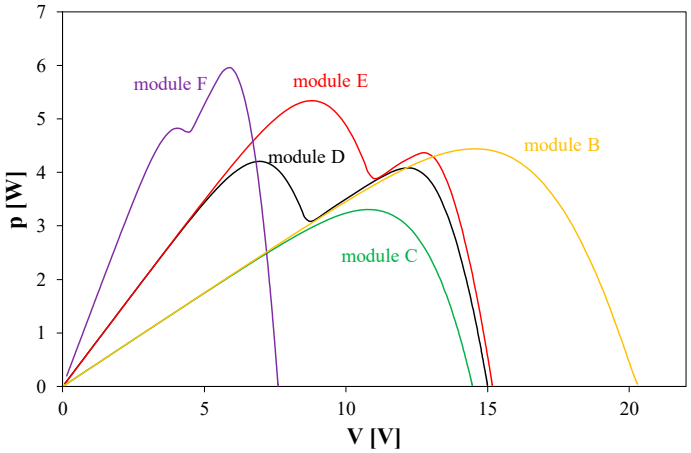

Figure 15. Dependence of the power produced on the voltage for the tested modules with the shading of a single solar cell in each module.

For module A, shading of one solar cell caused the entire module to lose its ability to generate electricity (the graph coincides with the voltage axis). The remaining modules, thanks to the use of parallel-connected solar cell strings or bypass diodes, generated electricity in these conditions. However, the p(V) characteristics differed significantly from the characteristics obtained in the absence of shading.

The characteristics visible in Figure 15 had a different course for each module. The p(V) dependence had one maximum for modules B and C, while for the remaining modules, two local maxima were visible. For each module, these maxima occurred at a different voltage value. The lowest voltage was obtained for module F (approx. 6 V), and the highest (approx. 15 V) for module B. The maximum power values obtained for individual modules ranged from 3.2 W (for module C) to 6 W (for module F).

Another example concerns the tested modules operating with shading of two solar cells in the module. These were selected in such a way that, for each of the modules, it was the most unfavourable variant. This means that each of the shading solar cells was located in a different string. It caused these strings to be unable to generate power. The obtained analysis results are presented in Figure 16.

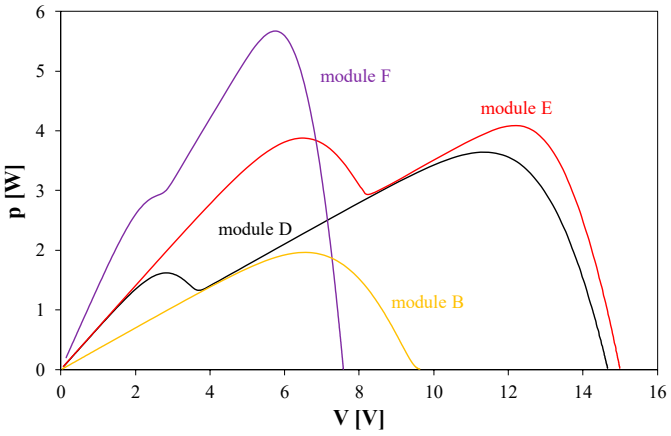

Figure 16. Dependence of the produced power on the voltage for the tested modules with unfavourable shading of two solar cells in the modules.

In this shading variant, modules A and C did not generate electricity. Therefore, their characteristics are not visible. In comparison with the previously considered cases, it can be seen that the open-circuit voltage value decreased.

The presented p(V) dependences showed single or double maxima. The maximum values of the generated power were the smallest for module B and amounted to about

2 W, and the largest were for module F, amounting to 5.6 W. In comparison with the case presented in Figure 15, it can be seen that the maximum power value decreased the least for module F. This proves that it is possible to limit the reduction in the value of the generated power due to shading by connecting solar cells in the panel into short strings, which are bypassed by other solar cell strings and bypass diodes.

On the basis of the performed analyses, it is visible that, with the use of module F, it is possible to obtain the highest value of generated power. The block diagram of this module is shown in Figure 17.

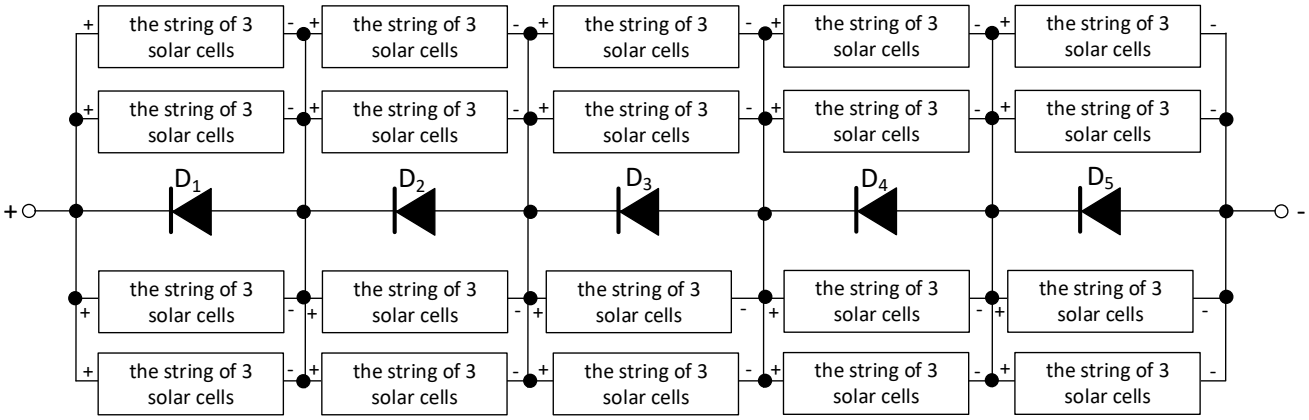

Figure 17. Network representation of the connections in module F.

7. Conclusions

Using the proposed PV module model, the I-V and P-V characteristics of the considered constructions of the PV modules were calculated under different shading conditions. Some of these characteristics were also measured. In all considered cases, good modelling accuracy of the considered characteristics was obtained. This demonstrates the correctness of the developed model. Additionally, the presented characteristics illustrate the advantages of half-cut PV modules that enable the generation of photocurrent even when their surfaces are partially shaded. These characteristics indicate that, in partial shade conditions, the characteristics of the considered modules have shapes significantly different from the typical shapes of first- and second-generation solar modules. On the other hand, it was shown that, due to the breakdown in the p-n junction of the solar cells, the power could be also generated in PV modules of classical construction. These results also prove that the number of solar cells used in one string is limited by the value of breakdown voltage of the solar cells used.

As a result of the calculations carried out for various PV module designs, it was found that in the absence of shading, there were no significant differences between the characteristics of individual modules. The differences became clear when at least one solar cell was shaded. Then, for the classic PV module design, no electricity production was observed, and for the other designs, a decrease in the maximum power value was visible. The greater the number of sections the panel was divided into, the smaller the power decrease. In the case of shading two solar cells, their locations on the module were important. However, it can be seen that the maximum power generated by a partially shaded module was a decreasing function of the number of solar cell strings in the module under consideration. For example, dividing the module into 20 areas creating such strings meant that shading any number of solar cells from this string would cause a decrease of only 15%, in the value of the maximum generated power while using a classic design of such a module would reduce the value of the generated power practically to zero.

The PV module model proposed in this paper and the presented calculation and measurement results may be useful for designers of PV modules, as well as installations. They can help with the optimal division of the module into sections and reduce power losses due to shading. They can also be used in teaching to illustrate the impact of shading

different sections of PV modules on their characteristics and the power that can be obtained from them.

Author Contributions: Conceptualization, E.K., K.G. and J.D.; methodology, E.K., K.G. and J.D.; investigation, E.K. and K.G.; resources, J.D.; writing—original draft preparation, E.K. and K.G.; writing—review and editing, E.K., K.G. and J.D.; visualization, E.K. and K.G.; supervision, K.G. All authors have read and agreed to the published version of the manuscript.

Funding: This research received no external funding.

Data Availability Statement: The presented experimental data can be made available upon request.

Conflicts of Interest: The authors declare no conflicts of interest.

References

1. Sopian, K.; Cheow, S.L.; Zaidi, S.H. An overview of crystalline silicon solar cell technology: Past, present, and future. *AIP Conf. Proc.* **2017**, *1877*, 020004.
2. Rashid, M.H. *Power Electronic Handbook*; Academic Press: Cambridge, MA, USA; Elsevier: Amsterdam, The Netherlands, 2007.
3. Castaner, L.; Silvestre, S. *Modelling Photovoltaic Systems Using Pspice*; John Wiley & Sons: Hoboken, NJ, USA, 2002.
4. Hemza, A.; Abdeslam, H.; Chenni, R.; Narimene, D. Photovoltaic system output simulation under various environmental conditions. In Proceedings of the International Renewable and Sustainable Energy Conference (IRSEC), Marrakech, Morocco, 14–17 November 2016; pp. 722–726.
5. Matuszczyk, P.; Popławski, T.; Flasza, J. Wpływ natężenia promieniowania słonecznego i temperatury modułu na wybrane parametry i moc znamionową paneli fotowoltaicznych [The influence of solar radiation and temperature module on selected parameters and the power rating of photovoltaic panels]. *Przegląd Elektrotechniczny* **2015**, *91*, 159–162. [CrossRef]
6. Górecki, K.; Dąbrowski, J.; Krac, E. SPICE-aided modeling of daily and seasonal changes in properties of the actual photovoltaic installation. *Energies* **2021**, *14*, 6247. [CrossRef]
7. Eduardo, M.; Godinho, R.; Radu, G.; Mousa, M.; Edris, P. Simulation and Comparison of Mathematical Models of PV Cells with Growing Levels of Complexity. *Energies* **2018**, *11*, 2902. [CrossRef]
8. Sarkar, M. Effect of various model parameter on solar photovoltaic cell simulation: A SPICE analysis. *Renew. Wind Water Sol.* **2015**, *3*, 1–9. [CrossRef]
9. Bąk, A.; Borowiecka, I.; Cierlicki, T.; Kruszelnicka, W. *Wpływ Warunków Środowiskowych na Wydajność Modułów Fotowoltaicznych*; Nr I–IV; Nauka Technika, Polska Energetyka Słoneczna: Warshaw, Poland, 2018; pp. 9–14.
10. Dąbrowski, J.; Krac, E.; Górecki, K. Analiza długookresowej wydajności instalacji fotowoltaicznej [Analysis of long-time efficiency of photovoltaic installation]. *Przegląd Elektrotechniczny* **2017**, *93*, 202–205.
11. Górecki, K.; Górecki, P.; Krac, E. Modelling simple photovoltaic systems with thermal phenomena taken into account. In Proceedings of the 23rd International Conference Mixed Design of Integrated Circuits and Systems, MIXDES 2016, Łódź, Poland, 23–25 June 2016; pp. 276–281.
12. Bidram, A.; Davoudi, A.; Balog, R.S. Control and Circuit Techniques to Mitigate Partial Shading Effects in Photovoltaic Arrays, Photovoltaics. *IEEE J. Photovolt.* **2012**, *2*, 532–546. [CrossRef]
13. Bizzarri, F.; Bongiorno, M.; Brambilla, A.; Gruosso, G.; Gajani, G.S. Model of photovoltaic power plants for performance analysis and production forecast, Sustainable Energy. *IEEE Trans. Energy Convers.* **2013**, *4*, 278–285. [CrossRef]
14. Villa LF, L.; Picault, D.; Raison, B.; Bacha, S.; Labonne, A. Maximizing the Power Output of Partially Shaded Photovoltaic Plants Through Optimization of the Interconnections Among Its Modules. *IEEE J. Photovolt.* **2012**, *2*, 154–163. [CrossRef]
15. Lameirinhas, R.; Torres, J.P.; Cunha, J. A Photovoltaic Technology Review: History, Fundamentals and Applications. *Energies* **2022**, *15*, 1823. [CrossRef]
16. Maciąg, K.; Maciąg, M. *Energetyka na Skalę XXI w.–Osiągnięcia i Perspektywy*; Wydawnictwo Naukowe TYGIEL: Lublin, Poland, 2018.
17. Novoselov, K.S.; Geim, A.K.; Morozov, S.V.; Jiang, D.; Zhang, Y.; Dubonos, S.V.; Grigorieva, I.V.; Firsov, A.A.; Novoselov, K.S. Electric field effect in atomically thin carbon films. In *Science, New Series Gene Expression: Genes in Action*; Phys.org: Isle of Man, UK, 2007; Volume 306, pp. 183–191.
18. Berger, C.; Song, Z.; Li, T.; Li, X.; Ogbazghi, A.Y.; Feng, R.; Dai, Z.; Marchenkov, A.N.; Conrad, E.H.; First, P.N.; et al. Ultrathin Epitaxial Graph-ite: 2D Electron Gas Properties and a Route Toward Graphene-based Nanoelectronics. *J. Phys. Chem. B* **2004**, *108*, 19912–19916. [CrossRef]
19. Haedrich, I.; Eitner, U.; Wiese, M.; Wirth, H. Unified methodology for determining CTM ratios: Systematic prediction of module power. *Sol. Energy Mater. Sol. Cells* **2014**, *131*, 14–23. [CrossRef]
20. Haberlin, H. *Photovoltaics. System Design and Practice*; Wiley: Hoboken, NJ, USA, 2012.
21. Champion Photovoltaic Module Efficiency Chart. Available online: https://www.nrel.gov/pv/module-efficiency.html (accessed on 8 October 2024).
22. LR4-72HPH 425–455 M Datasheet. Available online: https://natec.com/wp-content/uploads/2020/04/Datasheet-Longi-Solar-Mono-Silver-Frame-LR4-72HPH-425-455M-Hi-Mo4.pdf (accessed on 11 November 2024).

23. Shah, N.; Shah, A.A.; Leung, P.K.; Khan, S.; Sun, K.; Zhu, X.; Liao, Q. A Review of Third Generation Solar Cells. *Processes* **2023**, *11*, 1852. [CrossRef]
24. Znajdek, K.; Sibiński, M. *Postępy w Fotowoltaice*; Wydawnictwo Naukowe PWN: Lublin, Poland, 2021.
25. Hanifi, H.; Schneider, J.; Bagdahn, J. Reduced shading effect on half-cell modules–measurement and simulation. In Proceedings of the 31st European Photovoltaic Solar Energy Conference and Exhibition, Hamburg, Germany, 14–17 September 2018; pp. 2529–2533.
26. Mittag, A.; Pfreundt, J.; Shahid, N.; Wöhrle, D.; Neuhaus, D. Techno-economic analysis of half cell modules—The impact of half cells on module power and costs. In Proceedings of the 36th EU PV Solar Energy Conference and Exhibition, Marseille, France, 9–13 September 2019.
27. Górecki, K.; Krac, E. Wpływ sposobu połączenia fotoogniw w panelu fotowoltaicznym na jego odporność na częściowe zacienienie [The influence of the manner of connecting photocells in a photovoltaic panel on its resistance to partial shading]. *Przegląd Elektrotechniczny* **2024**, *100*, 246–249.
28. Gow, J.A.; Manning, C.D. Development of a photovoltaic array model for use in power electronics simulation studies. *IEEE Proc.* **1999**, *146*, 193–200. [CrossRef]
29. Soon, J.J.; Low, K.-S.; Goh, S.T. Multi-dimension diode photovoltaic (PV) model for different PV cell technologies. In Proceedings of the 2014 IEEE 23rd International Symposium on Industrial Electronics (ISIE), Gdańsk, Poland, 1–4 June 2014; pp. 2496–2501.
30. Díaz-Bernabé, J.L.; Morales-Acevedo, A. Photovoltaic module simulator implemented in SPICE and Simulink. In Proceedings of the 2015 12th International Conference on Electrical Engineering, Computing Science and Automatic Control (CCE), Mexico City, Mexico, 28–30 October 2015; pp. 1–5.
31. Dimitrijević, M.; Stosovic, M.; Litovski, V. An MPPT controller model for a standalone PV system. *Int. J. Electron.* **2020**, *107*, 1345–1363. [CrossRef]
32. Evstatiev, B.I.; Codreanu, N.D.; Gabrovska-Evstatieva, K.G. Virtual investigations of a stand-alone photovoltaic system with supercapacitor bank used to power an irrigation system. In Proceedings of the 2020 IEEE 26th International Symposium for Design and Technology in Electronic Packaging (SIITME), Pitesti, Romania, 21–24 October 2020; pp. 421–425.
33. Gadjeva, E.; Hristov, M. Behavioral parametrized SPICE models of photovoltaic modules. In Proceedings of the 20th International Conference Mixed Design of Integrated Circuits and Systems MIXDES, Gdynia, Poland, 20–22 June 2013; pp. 355–359.
34. Gadjeva, E.; Hristov, M. Computer-aided model parameter extraction of photovoltaic modules using SPICE. In Proceedings of the 2017 International Symposium on Power Electronics (Ee), Novi Sad, Serbia, 19–21 October 2017; pp. 1–5.
35. Górecki, K.; Dąbrowski, J.; Krac, E. Modeling solar cells operating at waste light. *Energies* **2021**, *14*, 2871. [CrossRef]
36. Gontean, A.; Septimiu, L.; Bularka, S.; Szabo, R.; Lascu, D. A Novel High Accuracy PV Cell Model Including Self Heating and Parameter Variation. *Energies* **2018**, *11*, 36. [CrossRef]
37. Lyden, S.; Haque, M.E.; Gargoom, A.; Negnevitsky, M.; Muoka, P.I. Modelling and parameter estimation of photovoltaic cell. In Proceedings of the 22nd Australasian Universities Power Engineering Conference (AUPEC), Bali, Indonesia, 26–29 September 2012; pp. 1–6.
38. Abdulrazzaq, A. Electro-thermal modeling of photovoltaic (PV) systems. In Proceedings of the Spring Wind 2018, Györ, Hungary, 3–5 May 2019.
39. Dąbrowski, J.; Krac, E.; Górecki, K. New model of solar cells for SPICE. In Proceedings of the 25th International Conference Mixed Design of Integrated Circuits and Systems MIXDES 2018, Gdynia, Poland, 21–23 June 2018; pp. 338–342.
40. Guo, S.; Singh, J.P.; Peters, I.M.; Aberle, A.G.; Walsh, T.M. A Quantitative Analysis of Photovoltaic Modules Using Halved Cells, Hindawi Publishing Corporation. *Int. J. Photoenergy* **2013**, *2013*, 8. [CrossRef]
41. Joshi, A.; Khan, A.; Sp, A. Comparison of half cut solar cells with standard solar cells. In Proceedings of the 2019 Advances in Science and Engineering Technology International Conferences (ASET), Dubai, United Arab Emirates, 26 March–10 April 2019; pp. 1–3. [CrossRef]
42. Rodacki, T.; Kandyba, A. *Przetwarzanie Energii w Elektrowniach Słonecznych*; Wydawnictwo Politechniki Śląskiej: Warshaw, Poland, 2000.
43. Ramos, C.A.F.; Alcaso, A.N.; Cardoso, A.J.M. Photovoltaic-thermal (PVT) technology: Review and case study. *IOP Conf. Ser. Earth Environ. Sci.* **2019**, *354*, 012048. [CrossRef]
44. Górecki, K.; Krac, E. Measurements of thermal parameters of a solar module. *J. Phys. Conf. Ser.* **2016**, *709*, 012007. [CrossRef]
45. Górecki, K.; Górecki, P.; Paduch, K. Modelling solar cells with thermal phenomena taken into account. *J. Phys. Conf. Ser.* **2014**, *494*, 012007. [CrossRef]
46. Wilamowski, B.; Jager, R.C. *Computerized Circuit Analysis Using SPICE Programs*; McGraw-Hill: New York, NY, USA, 1997.
47. Solar Cell Data Sheet. Available online: https://www.conrad.fr/fr/p/velleman-sol1n-module-solaire-polycristallin-0-5-v-1713847.html (accessed on 11 November 2024).
48. Axial Lead Rectifiers, Schottky Barrier Rectifiers 1N5817, 1N5818, 1N5819, ONsemi, Datasheet. Available online: https://www.onsemi.com/download/data-sheet/pdf/1n5817-d.pdf (accessed on 11 November 2024).